Cellular/Molecular

Reactivation of Early-Life Stress-Sensitive Neuronal Ensembles Contributes to Lifelong Stress Hypersensitivity

Julie-Anne Balouek, Christabel A. Mclain, Adelaide R. Minerva, Rebekah L. Rashford, Shannon N. Bennett, Forrest D. Rogers, and Catherine Jensen Peña

Princeton Neuroscience Institute, Princeton University, Princeton, New Jersey 08544

Early-life stress (ELS) is one of the strongest lifetime risk factors for depression, anxiety, suicide, and other psychiatric disorders, particularly after facing additional stressful events later in life. Human and animal studies demonstrate that ELS sensitizes individuals to subsequent stress. However, the neurobiological basis of such stress sensitization remains largely unexplored. We hypothesized that ELS-induced stress sensitization would be detectable at the level of neuronal ensembles, such that cells activated by ELS would be more reactive to adult stress. To test this, we leveraged transgenic mice to genetically tag, track, and manipulate experience-activated neurons. We found that in both male and female mice, ELS-activated neurons within the nucleus accumbens (NAc), and to a lesser extent the medial prefrontal cortex, were preferentially reactivated by adult stress. To test whether reactivation of ELS-activated ensembles in the NAc contributes to stress hypersensitivity, we expressed hM4Dis receptor in control or ELS-activated neurons of pups and chemogenetically inhibited their activity during experience of adult stress. Inhibition of ELS-activated NAc neurons, but not control-tagged neurons, ameliorated social avoidance behavior following chronic social defeat stress in males. These data provide evidence that ELS-induced stress hypersensitivity is encoded at the level of corticolimbic neuronal ensembles.

Key words: **DREADDs; early life adversity; early life stress; engram; nucleus accumbens (NAc); social defeat**

Significance Statement

Early-life stress enhances sensitivity to stress later in life, yet the mechanisms of such stress sensitization are largely unknown. Here, we show that neuronal ensembles in corticolimbic brain regions remain hypersensitive to stress across the life span, and quieting these ensembles during experience of adult stress rescues stress hypersensitivity.

Introduction

Experience of early-life stress (ELS) is a major risk factor for mood and anxiety disorders later in life, with an effect size that far outweighs any known genetic risk (Green et al., 2010; Scott et al., 2012). In humans and animals, ELS sensitizes individuals to stress later in life, leading to a first appearance or synergistic worsening of depression-like symptoms after additional stress (McLaughlin et al., 2010; Zhang et al., 2016; Peña et al., 2017, 2019; Saxton and Chyu, 2020; Sidamon-Eristoff et al., 2022). The brain is particularly sensitive to environmental experiences when it is rapidly developing early in life, and there may be sensitive windows when childhood adversity increases vulnerability to depression (Dunn et al., 2018, 2019). However, the cellular mechanisms linking early adverse experience with enhanced sensitivity to stress and vulnerability to psychiatric disease remain largely unknown.

Experience of an event facilitates the formation or strengthening of cellular ensembles that are reactivated during recall of the experience (Han et al., 2009; Liu et al., 2012; Deng et al., 2013; Ramirez et al., 2013; Josselyn et al., 2015; Ryan et al., 2015; Tonegawa et al., 2015a,b; Cai et al., 2016; Kitamura et al., 2017; Pignatelli et al., 2019). In addition to pioneering findings in hippocampus (Guzowski et al., 1999; McKenzie et al., 2014), subsequent studies have also shown the sufficiency, necessity, and correlation of putative neuronal ensembles for a fear memory in several other brain structures including regions of the amygdala, medial prefrontal cortex (mPFC), and hypothalamus, demonstrating that cell ensembles for a given memory are not restricted to a single brain region but may be dispersed throughout the brain (Han et al., 2007; Cowansage et al., 2014; Butler et al., 2015; Janak and Tye, 2015; Ryan et al., 2015; Davis and Reijmers, 2018; Matos et al., 2019; Roy et al., 2022). Moreover, distinct types of memory, such as fear, reward, and social memories, are encoded

Received Jan. 3, 2023; revised June 1, 2023; accepted June 17, 2023.

Author contributions: J.-A.B. and C.J.P. designed research; J.-A.B., C.A.M., A.R.M., R.L.R., S.N.B., F.D.R., and C.J.P. performed research; J.-A.B. and C.J.P. analyzed data; J.-A.B. and C.J.P. wrote the paper.

This research was funded by National Institutes of Health Grants R00-MH-115096 (C.J.P.) and R01-MH-129643 (C.J.P.); PNI (Princeton Neuroscience Institute) Research Innovator Award (C.J.P.); and the New York Stem Cell Foundation (C.J.P.). C.J.P. is a New York Stem Cell Foundation Robertson Investigator. We thank Dr. Abigail Polter for helpful early discussion, and Tanzina Islam and Dana Waitman for their assistance with images. Parts of some figures were generated with BioRender.com.

The authors declare no competing financial interests.

Correspondence should be addressed to Catherine Jensen Peña at cpena@princeton.edu.

https://doi.org/10.1523/JNEUROSCI.0016-23.2023

in distinct ensembles within the brain (Hsiang et al., 2014; McKenzie et al., 2014; Redondo et al., 2014; Okuyama et al., 2016; Zhou et al., 2019; Shpokayte et al., 2022). Reactivation of ensembles associated with either positive or negative valence experiences is sufficient to drive preference or aversion in a reversible manner (Shpokayte et al., 2022), and ablating or inhibiting fear-associated ensembles erases their associated fear memories (Han et al., 2009; Denny et al., 2014). We hypothesized that one mechanism of ELS-induced stress hypersensitivity was through reactivation of ELS-sensitive cellular ensembles in mesocorticolimbic regions of the brain.

While there are many tools to record neuronal activity as it happens, until the last decade identifying and accessing cells activated by a distant past experience has been a major challenge in the field of neuroscience (DeNardo and Luo, 2017). To overcome this challenge, we took advantage of advances in mouse transgenics to genetically tag, track, and manipulate experience-activated cells in a temporally specific manner. Using transgenic mice (ArcCreER^{T2}) to indelibly label ELS-activated cells (Denny et al., 2014), we investigated the recruitment and reactivation of ELS-activated cellular ensembles during adult stress as indicated by fluorescent imaging of single-labeled and double-labeled cells throughout key mesocorticolimbic regions known to be sensitive to stress across the life span (Russo and Nestler, 2013; Hanson et al., 2021). We focused on the nucleus accumbens (NAc) and its neuromodulatory and glutamatergic inputs, including ventral tegmental area (VTA), basolateral amygdala (BLA), and mPFC. This allowed us to test the following two possible hypotheses: (1) that adult stress activates overall more neurons given a history of prior ELS; and (2) that ELS-activated cells are preferentially reactivated by adult stress. Finally, using Cre-dependent designer receptors exclusively activated by designer drugs (DREADDs) chemogenetic manipulation within these mice, we silenced ELS-activated ensembles in the NAc during adult stress to test whether cells initially activated by ELS contribute to behavioral hypersensitivity to future stress.

Materials and Methods

Mice

All protocols were performed in compliance with the *Guide for the Care and Use of Laboratory Animals* (NIH Publication 865–23) and were approved by the Institutional Animal Care and Use Committee of Princeton University (protocol #2135). Mice were housed in a temperature-controlled and humidity-controlled animal care facility with 12 h light/dark cycle (lights on at 12:00 A.M.) and were group housed in sets of three to five with *ad libitum* access to food and water. Mice were considered to be "male" or "female" based on external genitalia (adult) and/or anogenital distance (pups). For all experiments, mice were bred in-house in trios. Males were removed after 5 d, and females remained housed together until 19 d postmating, at which point females were individually housed in clean cages with nesting material from the previous cage for olfactory continuity to reduce stress. Litters were randomly assigned at birth to standard (Std)-rearing or ELS conditions, described below. All offspring were weaned at postnatal day 21 (P21) by sex. Both males and females were included in all experiments.

Transgenic mice were on a C57BL/6J background. Heterozygous *Arc-CreER*$^{T2/+}$ mice (Denny et al., 2014; stock #022357, The Jackson Laboratory) were bred with *R26-CAG-LSL-Sun1-sfGFP-Myc* knock-in mice ("Sun1-sfGFP"; stock #030952, The Jackson Laboratory; Mo et al., 2015) for imaging experiments. In this cross, recombination and expression of the *Sun1-sfGFP* transgene is activity-dependent and ligand-dependent. Activity-induced expression of the immediate early gene *Arc* drives expression of the CreERT2 fusion protein, which is sequestered in the cytoplasm until injection of a selective estrogen receptor modulator such as 4-hydroxytamoxifen (4-OHT). Administration of 4-OHT allows relocalization of CRE to the nucleus, where it can act as a recombinase to remove the floxed STOP cassette and allow permanent expression of the fusion SUN1-sfGFP protein. SUN1 is an inner nuclear membrane-spanning protein, such that SUN1-sfGFP becomes localized to the nuclear membrane of neurons activated during the duration of action of 4-OHT. Double-transgenic offspring were used for all imaging studies. Offspring of heterozygous *Arc-CreER*$^{T2/+}$ mice bred in-house with C57BL/6J wild-type mice were used for DREADD experiments. Wild-type C57BL/6J mice were used for DREADD ligand dose piloting studies. Retired Swiss-Webster male breeder mice (Taconic) were housed individually and used as aggressor mice in chronic nondiscriminatory social defeat stress (CNSDS).

Genotyping

Offspring genotyping was performed by toe clip within 1 d of birth. *Arc-CreER*$^{T2/+}$ × *Sun1-sfGFP* founders and subsequent offspring were genotyped using the following primer sets: *Cre*: 5'-GCC TGC ATT ACC GGT CGA TGC AAC G-3'; 5'-AAA TCC ATC GCT CGA CCA GTT TAG TTA CCC-3'; *Sun1-sfGFP* (mutant): 5'-CTG AAC TTG TGG CCG TTT AC-3'; 5'-ACA CTT GCC TCT ACC GGT TC-3'; wild-type: 5'-CAG GAC AAC GCC CAC ACA-3'; and 5'-AAG GGA GCT GCA GTG GAG TA-3′. Cre and Sun1-sfGFP genotypings were performed separately. Sun1-sfGFP genotyping was performed following The Jackson Laboratory genotyping protocol.

Early-life stress paradigm

ELS occurred from P10 to P17 as previously described (Peña et al., 2017, 2019) and consisted of both maternal separations (with all pups from a litter removed to a clean cage and returned to the home cage 3–4 h later) and limited nesting material in the home cage (to one-third of standard EnviroDri nesting puck size). Pups were given access to diet gel and several chow pellets on the cage floor during separations, although pups were not observed to eat anything. At the conclusion of ELS on P17, mice were given clean cages with a full puck of nesting material and were left undisturbed until weaning. Std facility-reared pups were reared with a normal amount of nesting material and left unhandled.

Administration of 4-hydroxytamoxifen

4-OHT (catalog #H7904, Sigma-Aldrich) was first prepared as 25 mg/ml stock solutions in ethanol and frozen at −2°C. For injections, 4-OHT was prepared fresh daily from stock to 5 mg/ml, dissolved in ethanol and corn oil (1:4). At P17, double-transgenic *Arc-CreER*$^{T2/+}$ × Sun1-GFP mice received intraperitoneal injections at 50 mg/kg body weight. Injections were given to ELS pups at the start of 4 h of maternal separation. To tag a specific, positive valence experience in standard-reared pups, pups were provided with a novel enrichment object (a plastic exercise saucer) in the home cage at P17 before 4-OHT administration. Pups were observed to explore the novel object but not necessarily run on it.

Adult stress: CNSDS

Both male and female mice were exposed to CNSDS (Yohn et al., 2019; Dieterich et al., 2021), a modified version of chronic social defeat stress (Berton et al., 2006) for simultaneous social stress of male and female mice. Briefly, beginning at age P60, CNSDS-assigned mice were subject to 10 d of daily social defeat by a Swiss Webster retired breeder ("aggressor"; Taconic) in a standard rat cage filled with corn cob bedding. An experimental male mouse was introduced to the cage of an aggressor first for ~3 min, followed by an experimental female mouse for an additional 5 min. Males were then moved across a perforated Plexiglas barrier within the aggressor cage, while females were single-housed with a handful of soiled aggressor bedding (imaging experiments) or were cohoused in a new cage across a Plexiglas barrier from a different aggressor (DREADD experiments). Experimental mice were introduced to a new aggressor each day for 10 d, and males and females were rotated in different directions so that trios were unique each day. Control mice were housed in a standard mouse cage in pairs of the same sex, separated by a perforated Plexiglas barrier. For imaging experiments, mice were sacrificed 1 h after the last bout of social defeat.

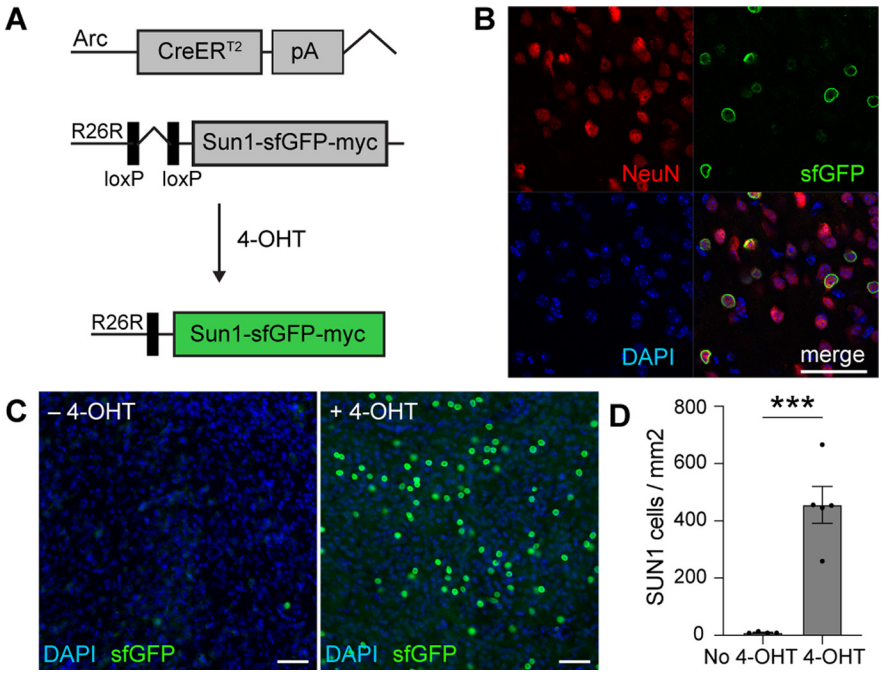

Figure 1. Validation of activity-dependent transgenic mice show neuronal specificity and low leak. ***A***, Schematic for 4-OHT-dependent and Arc expression-dependent recombination and transgene expression in double-transgenic Arc-CreERT2/+ × Sun1-sfGFP mice. ***B***, Representative 63× image within NAc of Arc-CreERT2/+ × Sun1-sfGFP mice after recombination, labeling all cells (DAPI), all neurons (NeuN), and previously activated cells (sfGFP). Scale bar, 50 µm. ***C***, Representative 20× images within NAc of Arc-CreERT2/+ × Sun1-sfGFP adult mice without (left) or with (right) prior 4-OHT administration at P17 show that spontaneous recombination without 4-OHT (leak) is low. Scale bar, 50 µm. ***D***, Quantification of GFP$^+$ cell density in double-transgenic mice with or without prior 4-OHT-induced recombination. Data are mean ± SEM. ***$p < 0.001$.

Mice in the DREADD experiment underwent CNSDS twice (see Fig. 5*C*). In the first round, all mice received an intraperitoneal vehicle injection of normal saline 30 min before social defeat or handling (control mice). In the second round, all mice received ligand injection (see below) 30 min before social defeat or handling. Notably, for DREADD experiments, both male and female experimental mice were only cohoused with aggressors for a maximum of 4 h after each day of social defeat to account for the 3–5 h functional period of olanzapine (OLZ; Mattiuz et al., 1997; Aravagiri et al., 1999) so that the presence of the aggressor did not continue to stress mice after DREADD inhibition of neurons was expected to wear off. At the conclusion of each round of CNSDS, male and female mice were individually housed in clean cages for the duration of behavior testing.

Immunohistochemistry and imaging

Mice were sacrificed 1 h after the last bout of early-life stress (see Fig. 2) or adult stress (see Figs. 3, 4) to capture maximal stress-induced c-Fos levels. An additional four adult *Arc-CreER$^{T2/+}$* × Sun1-sfGFP mice that never received 4-hydroxytamoxifen were sacrificed directly from the home cage to assess the background "leak" of Sun1-GFP expression (Fig. 1). Mice were anesthetized with ketamine/xylazine (100 and 10 mg/kg, i.p.) and transcardially perfused with sterile 1× PBS followed by 4% paraformaldehyde. Brains were removed, equilibrated in 30% sucrose in PBS, and frozen at −80°C until processing. Brains were sectioned in 50-µm-thick slices using a cryostat. Immunohistochemistry was performed using the following antibodies: c-Fos (clone9F6, mAb #2250, Cell Signaling Technology), GFP (catalog #GFP-1020, Aves Labs), tyrosine hydroxylase (catalog #22941, ImmunoStar), mCherry (DREADD; catalog #ab167453, Abcam), and Prolong Gold Antifade with DAPI (Thermo Fisher Scientific). Imaging was performed on a slide scanner (Nanozoomer 2.0HT, Hamamatsu). Detection, colocalization, and quantification were performed using ndpisplit (Deroulers et al., 2013) and ComDet v.0.5.3 plugin for FiJi/ImageJ (https://github.com/ekatrukha/ComDet) with the following parameters: pixel size, 12; intensity threshold for both channels, 9. For imaging data, each value is a mean of six traced ROIs for each animal on average (minimum of 2, maximum of 8), such that sample size is based on subjects rather than slices ($n = 8$ mice/group for validation imaging; 4–11 mice/group for reactivation imaging).

Behavioral testing

A within-subject design was used to test adult male and female behavior three times: first before CNSDS, after a first round of CNSDS with vehicle administration, and after a second round of CNSDS with DREADD ligand (see Fig. 5*C*).

Social interaction. To assess social avoidance behavior, experimental mice were tested in a two-stage social interaction test under red lighting, as previously described (Peña et al., 2017). Social avoidance has been previously associated with other depression-like behaviors and is responsive to antidepressant treatment (Berton et al., 2006; Krishnan et al., 2007). In the first 2.5 min stage, the experimental mouse was allowed to freely explore an arena (44 × 44 × 20 cm) containing a novel Plexiglas and wire mesh enclosure (novel object; 10 × 6 cm) centered against one wall of the arena. In the second 2.5 min stage, the experimental mouse was immediately returned to the arena with a novel Swiss Webster mouse (aggressor strain) within the enclosure. Time spent in the "interaction zone" (14 × 26 cm) surrounding the enclosure, "corner zones" (10 × 10 cm), and "distance traveled" within the arena was measured by video tracking software (Ethovision, Noldus). A social interaction ratio (SI Ratio) was calculated of time spent exploring the novel mouse over time exploring the novel object; mice were considered "susceptible" to CNSDS if the SI Ratio was <0.9, "resilient" if the SI Ratio was >1.1, and "indifferent" for the interaction scores in between. To combat habituation during repeated testing, patterns on the walls of the chambers were altered for each of the three testing sessions.

Open-field test. Mice were allowed to explore a brightly lit, empty arena (44 × 44 × 20 cm) for 10 min. Total distance traveled, velocity, and time spent in the center (20 × 20 cm) were recorded and measured via Ethovision (Noldus), as previously described (Peña et al., 2017). To combat habituation during repeated testing, patterns on the walls of the chambers were altered for each testing session.

Novelty-suppressed feeding. Novelty-suppressed feeding testing was adapted from previous work (Bodnoff et al., 1989). Mice were food deprived for 18 h in a clean homecage. On testing day, they were placed

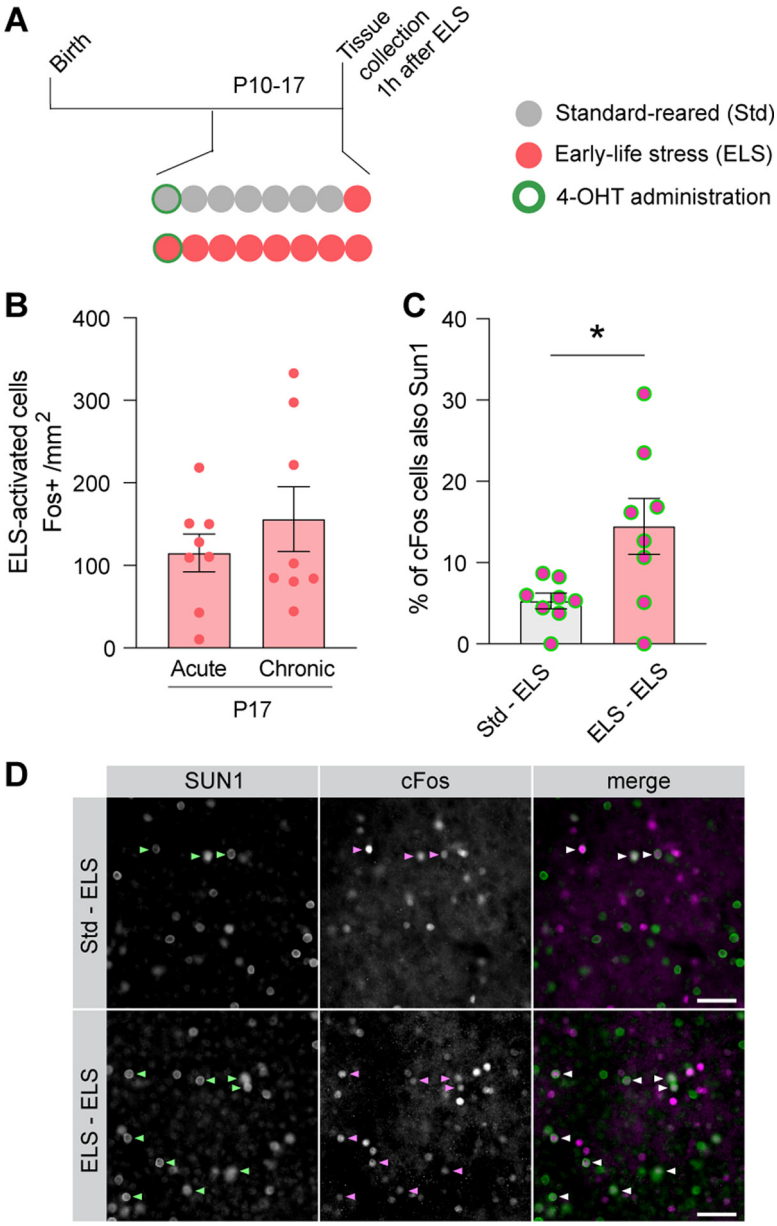

Figure 2. Experience-dependent neuronal labeling is specific. ***A***, Experiment design for assessing specificity and drift of ELS activity: genetic recombination was induced with 4-OHT at P10, and tissue was collected on P17. Acute stress mice were presented with enrichment on the day of tagging at P10, and were reared in standard conditions then exposed to a single day of ELS on P17. Chronic stress mice were subjected to ELS daily from P10 to P17. ***B***, No changes were observed in the density of ELS-activated cells in NAc following either acute or chronic stress, as assessed by c-Fos$^+$ cell density in response to ELS at P17. ***C***, Quantification of the percentage of c-Fos$^+$ cells active in NAc during ELS at P17 that were also active (GFP$^+$) during either Std/enrichment or ELS at P10 revealed significantly greater reactivation under matched conditions (ELS-ELS) compared with unmatched conditions (reward vs ELS). ***D***, Representative images in NAc associated with ***C***. Scale bar, 50 µm. Data are mean ± SEM. *$p < 0.05$.

in a corner of a novel, brightly lit (200 lux) arena (44 × 44 × 20 cm). The floor was covered with corncob bedding, and the arena walls were covered with a geometric pattern to enhance the novelty of the environment. A single food pellet was attached to a white circular platform (diameter, 10 cm) in the center of the arena. The test lasted until mice took their first bite (sitting on their haunches and using their forepaws to hold and bite the pellet), or for a maximum of 10 min. Mice that timed out were assigned a latency of 600 s. Immediately after taking their first bite, mice were transferred to their home cages and given access to their usual amount of food. To combat habituation during repeated testing, patterns on the walls of the chambers were altered for each testing session.

Pharmacogenetic inhibition of cellular activity

DREADDs were used to suppress cellular activity. An adeno-associated virus (AAV) transgene expressing Cre-dependent inhibitory DREADDs (pAAV-hSyn-DIO-hM4D(Gi)-mCherry) was injected into NAc by aseptic intracranial stereotaxic surgery in ArcCreER^{T2} pups at postnatal day P7 [catalog #44362, Addgene (originally a gift from Bryan Roth; http://n2t.net/addgene:44362; Krashes et al., 2011]. All mice received hM4D (Gi) transgenes, and thus controls were within-mouse based on vehicle/ligand administration.

At P7, *Arc-CreER*$^{T2/+}$ pups were anesthetized with isoflurane (induction, 2–3%; maintenance, 1–2%) for surgeries and fitted into a dual-arm stereotaxic instrument with the nose fitted in the nose cone above the bite bar, and the head stabilized using blunt ends of ear bars between the ear and jaw. To bilaterally target the NAc, two Hamilton syringes were angled inward 7° and the following coordinates were used: mediolateral, ±1.4 mm; anteroposterior, 1.1 mm; dorsoventral, −4.2 mm. Two hundred nanoliters of AAV (2.5×10^{13}) were injected on each side. Both VetBond glue and two sterile sutures were used to ensure

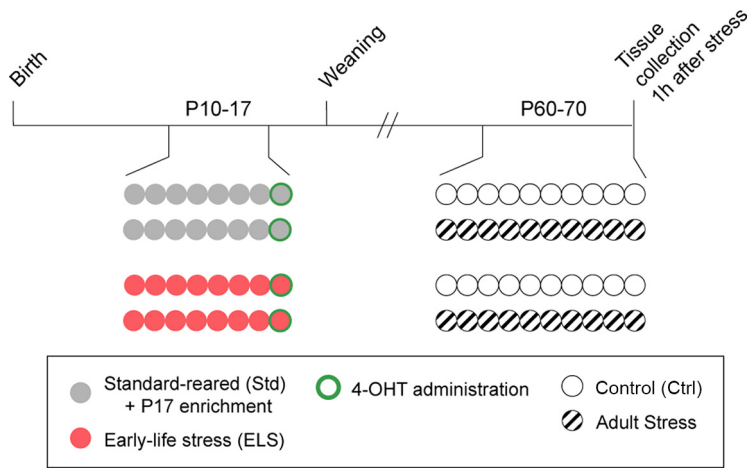

Figure 3. Experimental design for activity-dependent ELS engram labeling. Arc-CreERT2/+ × Sun1-sfGFP mice were either Std reared or experienced ELS from P10 to P17. Recombination was induced by 4-OHT administration on P17 prior to experience with a novel exercise saucer in the homecage (Std mice) or maternal separation (ELS). In adulthood, half of each group were assigned to 10 d of control conditions or CNSDS, and tissue was collected 1 h after the final bout of social defeat stress.

complete healing of incisions. Mice were given a perioperative topical dose of bupivacaine (0.25%, 2 mg/kg) and an additional dose 24 h following surgery. To prevent cannibalization of pups by dams following surgery, pups recovered in a partially warmed cage and dams were habituated with a piece of paper towel with sterile eye lubricant (Puralube Vet Ointment Sterile Ocular Lubricant, Dechra) and liquid tissue adhesive (VetBond, 3M); pups were only returned to the home cage with the dam once completely ambulatory. At P17, after 10 d of transgene expression, recombination was induced with 4-OHT as described above.

OLZ (Henry Schein Medical) was chosen as the hM4Di ligand for the inhibition of cellular activity as it has been shown to cross the blood–brain barrier, unlike the more common DREADD ligand clozapine *N*-oxide (CNO), and to be a specific and potent activator of hM4Di (Weston et al., 2019; Upright and Baxter, 2020). We sought to avoid CNO as it is back-converted to clozapine, which has unfavorable side effects in humans and may impact anxiety-like behavior at effective doses in mice. A dose of 0.1 mg/kg body weight OLZ was previously reported to be an effective ligand for hM4di DREADDs *in vivo* in mice (Weston et al., 2019). OLZ was prepared fresh daily from a −2°C stock and was diluted in normal saline to working concentrations (5 mg/ml). First, we tested two doses of OLZ (either 0.1 or 1.0 mg/kg body weight, i.p., given 30 min before behavioral testing) for a potential impact on anxiety-like and depression-like behavior and weight gain in wild-type C57BL/6J mice without hM4di expression ($n = 6$ male mice/group). A dose of 0.1 mg/kg body weight was selected for subsequent experiments based on a lack of impact on behaviors of interest in the absence of DREADDs. For DREADD inhibition experiments, both control and CNSDS mice were intraperitoneally administered vehicle (sterile normal saline) or 0.1 mg/kg OLZ 30 min before handling or social defeat, respectively, for the duration of CNSDS (10 d; 6–9 male and female mice/group).

Experimental design, data analysis, and statistics

All data are plotted as the mean ± SEM. We observed a small but significant effect of Sun1/+ versus Sun1/Sun1 genotype, with more cells counted in homozygous mice; to correct for this, *z*-scores of GFP^+ cells were calculated for Sun1/+ and Sun1/Sun1 genotypes separately. GFP and colocalization quantifications are thus presented as *z*-scores compared with the standard group. For imaging data, counts from two to six slices per subject were averaged, and the mean per subject was plotted and used for analysis, such that *n* represents individual subjects rather than replicate slices. All statistics were performed using SPSS (version 26) or Prism (version 9; GraphPad Software), with the α set to 0.05.

Four imaging experiments were performed to test (1) the degree of transgene leak (two-group comparison, $n = 4$–5/group); (2) the number of cells activated on the first versus the last day of ELS (two-group comparison, $n = 2$–3); (3) the specificity of early-experience cellular activity (two-group comparison, $n = 2$–3); and (4) the degree to which adult stress activated and reactivated cells depending on ELS history (2 × 2 experimental design, $n = 4$–11). Student's *t* test was used to compare two groups. Two-way ANOVA was used to test the main effects and interactions of early-life and adult stress.

Six groups were generated to test OLZ dose in a 2 × 3 design (vehicle and two doses, with and without stress, $n = 6$/group). Body weight was assessed using repeated-measures ANOVA, and the main effects/interactions of dose and stress were assessed using two-way ANOVA.

Behavioral effects of early life and adult stress were assessed using repeated-measures ANOVA given the within-animal repeated testing study design described above ($n = 6$–9/sex/group). *Post hoc* analyses between pairs of groups were conducted using Tukey's multiple-comparisons correction if there were significant main effects or interactions. Significant changes in proportion of resilient mice in the social avoidance task were calculated by two-tailed two-proportion *z*-test.

Data availability

All data and analysis code will be made available on request.

Results

Validation of activity-dependent transgenic mice

To validate whether our double-transgenic *Arc-CreER*$^{T2/+}$ × *Sun1-sfGFP* mice (Fig. 1*A*) allowed for an activity-dependent, ligand-dependent label with minimal background expression, we examined transgene expression with and without administration of 4-OHT in a homecage context. Administration of 4-OHT to Std-reared mice in adulthood produced superfolder GFP (sfGFP) localized to the nuclear membrane within 1 week. Consistent with known neuronal expression of Arc (Pastuzyn et al., 2018), all sfGFP-expressing cells colocalized with NeuN staining, confirming neuronal specificity (Fig. 1*B*). The absence of 4-OHT administration produced very little sfGFP expression even in adulthood, indicating low levels of spontaneous genetic recombination and "leakage" ($t_{(7)} = 6.103$, $p = 0.0005$, unpaired *t*-test; Fig. 1*C*,*D*).

Experience-dependent neuronal labeling is specific

Previous work has shown that rodents mount a comparable corticosterone response to maternal separation across days of separation, indicating a lack of habituation, but the extent to which mesocorticolimbic neuron activity might habituate to repeated

ELS was not yet known. To test this, and the specificity of activity labeling to experience, we administered 4-OHT to *Arc-CreER*$^{T2/+}$ × *Sun1-sfGFP* pups on P10 to label neurons during ELS or a distinct experience (homecage enrichment for 4 h in Std-reared mice). Pups continued to experience either ELS or Std conditions, and then all mice experienced ELS on P17 1 h before tissue collection (Fig. 2*A*). Quantification of c-Fos$^+$ cells in NAc on P17 1 h after experiencing ELS either for the first time ("acute") or the eighth time ("chronic") revealed similar levels of active neurons (Fig. 2*B*), indicating that mice do not habituate to ELS experience at the level of NAc activity.

We next sought to understand whether ELS activated the same ensembles of neurons across days, and the specificity of such activity. Quantification of the overlap of c-Fos$^+$ neurons activated by ELS on P17 that were previously active during P10 enrichment or P10 ELS revealed significantly greater reactivation under matched conditions ($t_{(14)} = 2.557$, $p = 0.0228$, unpaired *t*-test; Fig. 2*C*,*D*), suggesting the relative specificity and stability of ELS-sensitive ensembles in NAc, even after 1 week.

Mesocorticolimbic neurons activated by early-life stress, adult stress, or both

We next sought to investigate two possible hypotheses for how ELS-induced hypersensitivity to adult stress may be encoded at a cellular level: (1) that adult stress activates overall more neurons given a history of prior ELS; and (2) that ELS-activated cells are preferentially reactivated by adult stress. To test these hypotheses, we used *Arc-CreER*$^{T2/+}$ × *Sun1-sfGFP* mice and a 2 × 2 experimental design of ELS and/or adult CNSDS. With this design, Arc-driven SUN1-sfGFP expression represented cells active during specific early-life experience, and expression of the immediate early gene c-Fos at sacrifice represented cells active during adult experience (Fig. 3). To tag a specific positive-valence experience in Std-reared pups, and to tag a similar number of neurons in Std and ELS mice so as not to artificially bias the quantification of overlap, Std pups were given a novel enrichment object (a plastic exercise saucer) in the homecage at P17 before 4-OHT administration. We quantified the density of early-life (Std or ELS) activated GFP$^+$ cells, adult experience (control or CNSDS) activated c-Fos$^+$ cells, and their overlap across key stress-responsive mesocorticolimbic brain regions including NAc, mPFC, BLA, and VTA.

In all brain regions and analyses, there was no main effect of sex, and thus male and female samples were analyzed together. In all brain regions, we found similar densities of GFP$^+$ cells in response to Std and ELS on P17 (Fig. 4*A*,*E*,*I*,*M*). We also measured the percentage of DAPI-stained nuclei that were also GFP$^+$ and found no significant differences between Std and ELS mice within each region: 8.5% in NAc, 19.6% in PFC, 3.9% in BLA, and 3.1% in VTA (data not shown).

In NAc, we found a main effect of adult stress on c-Fos$^+$ cells ($F_{(1,27)} = 15.44$, $p = 0.0005$; Fig. 4*B*), density of colabeled cells ($F_{(1,27)} = 4.581$, $p = 0.042$; Fig. 4*C*), and percentage of early experience-activated cells that were reactivated by adult stress (trend level: $F_{(1,27)} = 3.610$, $p = 0.068$; Fig. 4*D*). There were also significant interactions between early-life and adult stress on activation (c-Fos$^+$ cells: $F_{(1,27)} = 5.339$, $p = 0.029$), density of colabeled cells ($F_{(1,27)} = 5.062$, $p = 0.033$), and percentage of early experience-activated cells that were reactivated by adult stress ($F_{(1,27)} = 4.367$, $p = 0.046$). Within ELS-reared mice, but not Std mice, *post hoc* analysis with Tukey's multiple-comparisons correction showed significant effects of adult stress on c-Fos$^+$ cellular density ($p < 0.0001$), density of colabeled cells ($p = 0.002$), and percentage of ELS-activated cells reactivated by adult stress ($p = 0.005$). Covarying for Sun1 and c-Fos in a GLM revealed that across all groups, reactivation was based strongly on c-Fos activity in adulthood ($p < 0.001$) and to a lesser degree on juvenile Sun1 tagging ($p = 0.122$). However, despite observing a higher degree of c-Fos$^+$ staining among Std-Control mice, we do not find a strong correlation between c-Fos and colocalization in this group (Std-Control, $R^2 = 0.079$; ELS-Control, $R^2 = 0.112$; Std-CNSDS, $R^2 = 0.852$; ELS-CNSDS, $R^2 = 0.563$), indicating that the relationship between c-Fos and colocalization only emerges with adult stress. Together, these results show a preferential activation (Fig. 4*B*) and reactivation (Fig. 4*C*,*D*) of ELS-activated cells by adult stress in NAc.

In mPFC, we observed that adult stress had a main effect on c-Fos$^+$ cells ($F_{(1,27)} = 12.28$, $p = 0.002$; Fig. 4*F*), colabeled cell density (trend-level: $F_{(1,27)} = 4.084$, $p = 0.053$; Fig. 4*G*), and the percentage of early experience-activated cells that were reactivated by adult stress ($F_{(1,27)} = 6.644$, $p = 0.016$; Fig. 4*H*). There was a trend for a main effect of ELS on mPFC ensemble reactivation ($F_{(1,27)} = 3.690$, $p = 0.065$). There were also interactions between early-life and adult stress on the activation (c-Fos$^+$ cells: $F_{(1,27)} = 7.261$, $p = 0.012$) and the percentage ($F_{(1,27)} = 5.888$, $p = 0.022$) of early experience-activated cells that were reactivated by adult stress. *Post hoc* analysis using Tukey's multiple-comparisons correction revealed significant effects of adult stress on c-Fos$^+$ cellular density ($p < 0.0001$), the density of colabeled cells ($p = 0.009$), and the percentage of ELS-activated cells reactivated by adult stress ($p = 0.0004$) in ELS-reared mice but not Std mice. In mPFC, we also found a significant difference in c-Fos$^+$ cells and the percentage of GFP$^+$ cells that were reactivated, between Std and ELS mice who have not experienced adult stress ($p = 0.022$ and $p = 0.017$, respectively). Together, these findings indicate that adult stress preferentially activates (Fig. 4*F*) and reactivates (Fig. 4*H*) ELS-activated cells in mPFC. However in mPFC, there was only a trending main effect of adult stress on colocalization (trend-level: $F_{(1,27)} = 4.084$, $p = 0.053$) and no interactions between early-life and adult experience on colocalization, in contrast to NAc.

In BLA, we found strong main effects of adult stress on c-Fos$^+$ cell density, colabeled cell density, and the proportion of early experience-activated cells that were reactivated by adult stress ($F_{(1,27)} = 24.27$, $p < 0.0001$; $F_{(1,27)} = 5.42$, $p = 0.028$; and $F_{(1,27)} = 8.441$, $p = 0.007$, respectively; Fig. 4*J*–*L*). There was a trend-level main effect of ELS on ensemble reactivation in BLA ($F_{(1,27)} = 4.091$, $p = 0.053$; Fig. 4*L*). Adult stress increased the density of c-Fos$^+$ cells in ELS mice ($p = 0.0002$) as well as in standard-reared mice (trend, $p = 0.051$; Fig. 4*J*). Adult stress also increased the density of colabeled cells ($p = 0.017$), and the percentage of ELS-activated cells reactivated by adult stress ($p = 0.008$) in ELS-reared mice but not in Std mice, as per a *post hoc* analysis using Tukey's multiple-comparisons correction. However, there were no significant interactions between early-life and adult stress within the BLA, indicating that while BLA strongly encodes recent adult stress experience, its activity may not encode a memory of prior ELS that contributes to stress sensitization.

Early-life or adult stress had no effect on overall c-Fos$^+$ activity in VTA (Fig. 4*N*) or ELS-activated cell reactivation (Fig. 4*O*, *P*). Of the reactivated cells in VTA, we also examined the proportion that were dopaminergic (overlap of TH$^+$, c-Fos$^+$, and

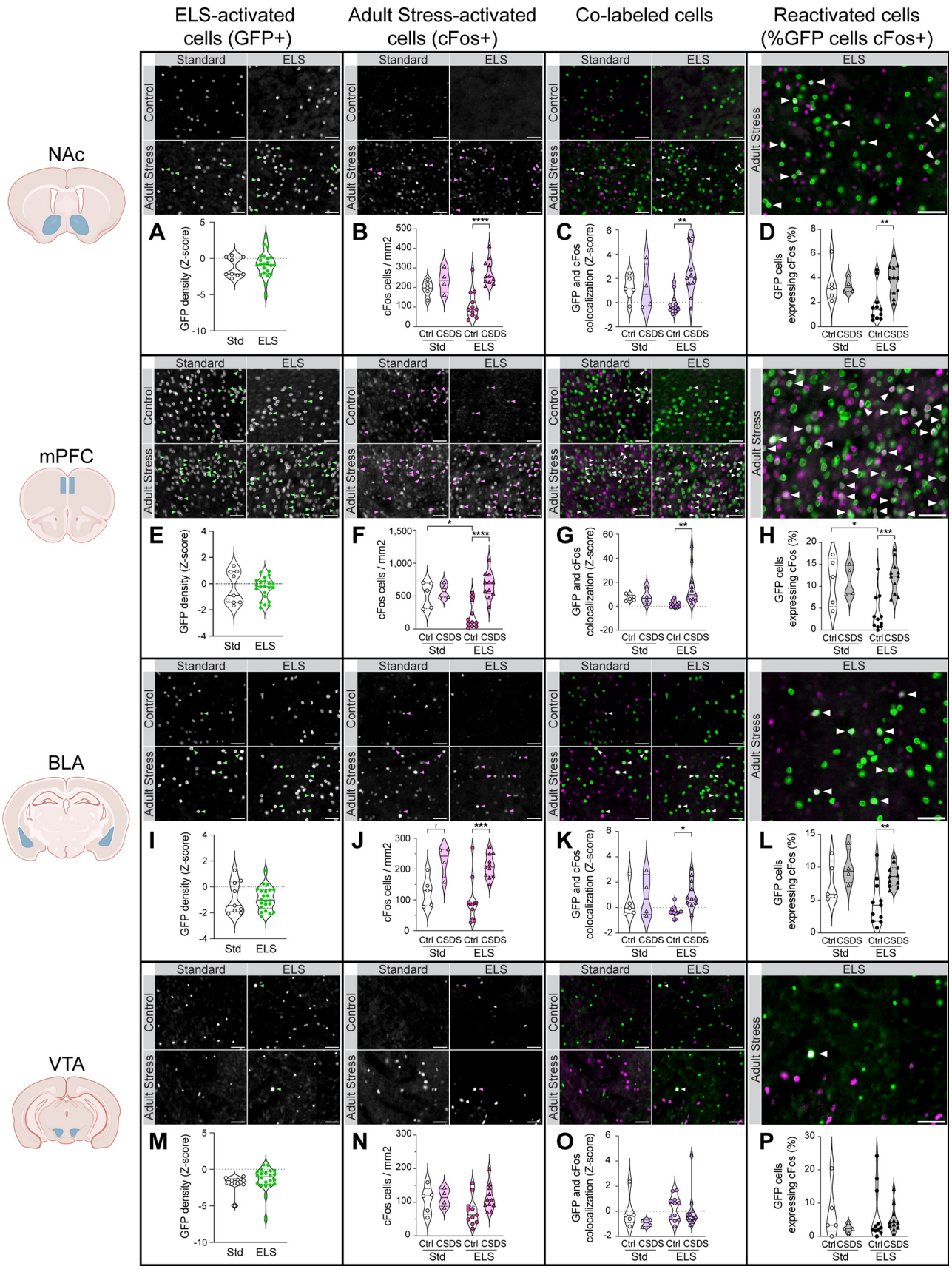

Figure 4. Stress-specific neuronal activation and reactivation in mesocorticolimbic brain regions. Each panel contains representative 20× images (scale bar, 50 μm) of mice from four groups (Std-Ctrl, ELS-Ctrl, Std-CNSDS, or ELS-CNSDS), and their quantification. Arrows indicate colocalized GFP$^+$ and c-Fos$^+$ cells. ***A–P***, The following four brain regions of the reward pathway were assessed: measures in NAc (***A–D***); measures in mPFC (***E–H***); measures in BLA (***I–L***); and measures in VTA (***M–P***). ***A***, ***E***, ***I***, and ***M*** show Std or ELS-activated cell density (GFP$^+$), presented as a *z*-score to correct for increased labeling in Sun1/Sun1 mice compared with Sun1/+ mice. ***B***, ***F***, ***J***, and ***N*** show control or CNSDS-activated cell density (c-Fos$^+$). ***C***, ***G***, ***K***, and ***O*** show a *z*-

sfGFP$^+$). We found that <10% of reactivated cells were dopaminergic, with no significant group differences (data not shown).

Chemogenetic inactivation of NAc ELS ensembles rescues behavioral hypersensitivity to adult social stress

Given that ELS-activated cells were preferentially reactivated by adult stress in NAc, we next sought to test whether reactivation of ELS-activated cells in NAc was functionally relevant for hypersensitivity to adult stress at the behavioral level using a chemogenetic approach (Peña et al., 2017). NAc also receives glutamatergic inputs from mPFC and BLA where we also found trending main effects of ELS on ensemble reactivation, making it an ideal region to target for functional manipulation. We hypothesized that inhibition of ELS-activated NAc neurons—but not a random subset of NAc neurons—during adult stress would alleviate hypersensitivity to the stressor on behavioral measures.

It was recently shown that olanzapine, a clinically approved antipsychotic drug with a more favorable side effect profile than clozapine, is a highly potent activator of hM4Di (Lieb et al., 2019; Weston et al., 2019; Upright and Baxter, 2020). OLZ also readily crosses the blood–brain barrier unlike the more common DREADD ligand CNO (Wang et al., 2004; Loryan et al., 2016; Gomez et al., 2017). Since the most common side effects of olanzapine are weight gain and drowsiness (Alper et al., 2007; van der Zwaal et al., 2014), we confirmed there was no effect of OLZ alone on weight or depression-like and anxiety-like behaviors before using it as a DREADD ligand in our behavioral studies. To examine this, adult male wild-type C57BL/6J mice were tested for baseline social avoidance and open-field exploration, administered intraperitoneal injections of saline, 0.1 mg/kg OLZ, or 1 mg/kg OLZ 30 min before CNSDS daily for 10 d, and were retested for the same behaviors (Fig. 5*A*). Neither dose of OLZ altered weight gain across the 10 d (Fig. 5*B*), which is consistent with other mouse work (Shertzer et al., 2010; Weston et al., 2019). Neither the social interaction test (Fig. 5*C*,*D*,*G*,*H*) nor the open-field test revealed any significant differences between mice injected with saline and either dose of OLZ (Fig. 5*E*,*F*,*I*,*J*). Although it appears that OLZ-treated mice spent less time in the center of an open field than vehicle-treated mice, it is important to note that mice were randomized to treatment without regard for open-field center time, which happened to differ at baseline, and the duration did not differ from the prestress test (Fig. 5*F*). We proceeded with a dose of 0.1 mg/kg OLZ based on previously published hM4di ligand efficacy at this dose (Weston et al., 2019).

To manipulate specific ELS-activated neuronal ensembles hypothesized to contribute to ELS-induced behavioral dysfunction, we injected AAV expressing a Cre-dependent inhibitory DREADD hM4di in NAc of *Arc-CreER$^{T2/+}$* pups at P7 and allowed virus to express for 10 d before inducing recombination in Std or ELS-activated neurons with 4-OHT (Fig. 6*A*–*C*). We then used a within-subject test design to assess behavior before adult stress, after CNSDS with vehicle for full experience of social stress, or after a second round of CNSDS with 0.1 mg/kg (i.p) OLZ to inhibit early-life experience-activated ensembles during social stress experience. We found a main effect of sex across behavior tests and analyzed sexes separately.

There was a significant interaction between ELS and CNSDS with treatment on social avoidance behavior among males (social interaction ratio: $F_{(2,22)} = 5.087$, $p = 0.0153$; Fig. 6*D*). CNSDS with vehicle treatment decreased the proportion of male mice categorized as resilient among ELS males ($z_{(1,12)} = 2.00$, $p = 0.045$), but not Std males ($z_{(1,12)} = 1.08$, $p = 0.280$) compared with pre-CNSDS testing levels within each group (Fig. 6*E*). DREADD inhibition with OLZ treatment compared with vehicle increased the proportion of ELS mice considered resilient ($z_{(1,12)} = 2.45$, $p = 0.014$), but not the proportion of resilient Std males ($p = 0.577$). These data replicate prior findings (Peña et al., 2017) of an interaction between ELS and adult stress such that two hits of stress increase social avoidance (Fig. 6*F*), and demonstrate the efficacy of DREADD inhibition of ELS-activated NAc ensembles for rescuing social avoidance behavior after the second round of CNSDS.

In a novelty-suppressed feeding test, all but one male (Std-OLZ) was observed to eat in the novel arena. Contrary to prior literature, adult stress did not increase latency to eat in the novel arena, and there were no main effects of or interactions between ELS and CNSDS with treatment (Fig. 6*G*). In an open-field test, there was a main effect of CNSDS and treatment on center time ($F_{(2,22)} = 77.48$, $p < 0.0001$), such that adult stress decreased center exploration. However, there was no interaction with ELS or rescue by DREADD inhibition of NAc ensembles.

We also examined the behavior of female mice. There were no main effects of, or interactions between, ELS and CNSDS with DREADD inhibition on novelty-suppressed feeding or social avoidance behavior (Fig. 6*J*,*K*). However, female mice spend less time in the center of an open-field arena after each round of CNSDS (main effect of CNSDS and treatment: $F_{(2,22)} = 6.388$, $p = 0.007$), indicating that CNSDS was an effective stress in females (Fig. 6*L*). *Post hoc* analysis shows a decrease in open-field center time earlier among ELS females ($p = 0.055$, $p = 0.040$ for each respective round of defeat), than Std females ($p = 0.492$, $p = 0.079$ for each respective round of defeat).

Discussion

There is a critical gap in our understanding of the mechanisms by which ELS sensitizes the response to future stressors. We sought to investigate whether this hypersensitivity arose from the overactivation of stress-responsive brain regions broadly, or from activity within specific ensembles of ELS-responsive neurons. To overcome the challenge of identifying neurons active during a past experience, we leveraged *Arc-CreER^{T2}* transgenic mice to permanently label early experience-activated neurons and track them across the life span. We first showed that neuronal ensembles in NAc respond to distinct early-life experiences (Fig. 2*C*). We then showed that, while adult stress activated neurons in NAc, mPFC, and BLA more strongly than a control experience, these regions were not simply hyperactive in mice with prior ELS experience compared with standard-reared mice (Fig. 4). Instead, adult stress preferentially reactivated ELS-activated cells in both NAc and mPFC (Fig. 4), supporting our second hypothesis that specific ensembles of ELS-activated neurons contribute to lifelong stress hypersensitivity. Finally, inhibiting ELS-activated NAc neurons, but not control-tagged neurons, rescued social avoidance behavior in male mice following adult stress (Fig. 6). These findings suggest that ELS-activated neuronal ensembles in corticolimbic brain regions remain hypersensitive

←

score of the density of colabeled cells (GFP$^+$ and c-Fos$^+$). ***D***, ***H***, ***L***, and ***P*** show the percentage of Std or ELS-activated cells that were reactivated during adult stress [100 * (GFP$^+$ and c-Fos$^+$)/GFP$^+$]. Data are mean ± SEM. $^{\dagger}p < 0.01$, $^{*}p < 0.05$, $^{**}p < 0.01$, $^{***}p < 0.001$, $^{****}p < 0.0001$.

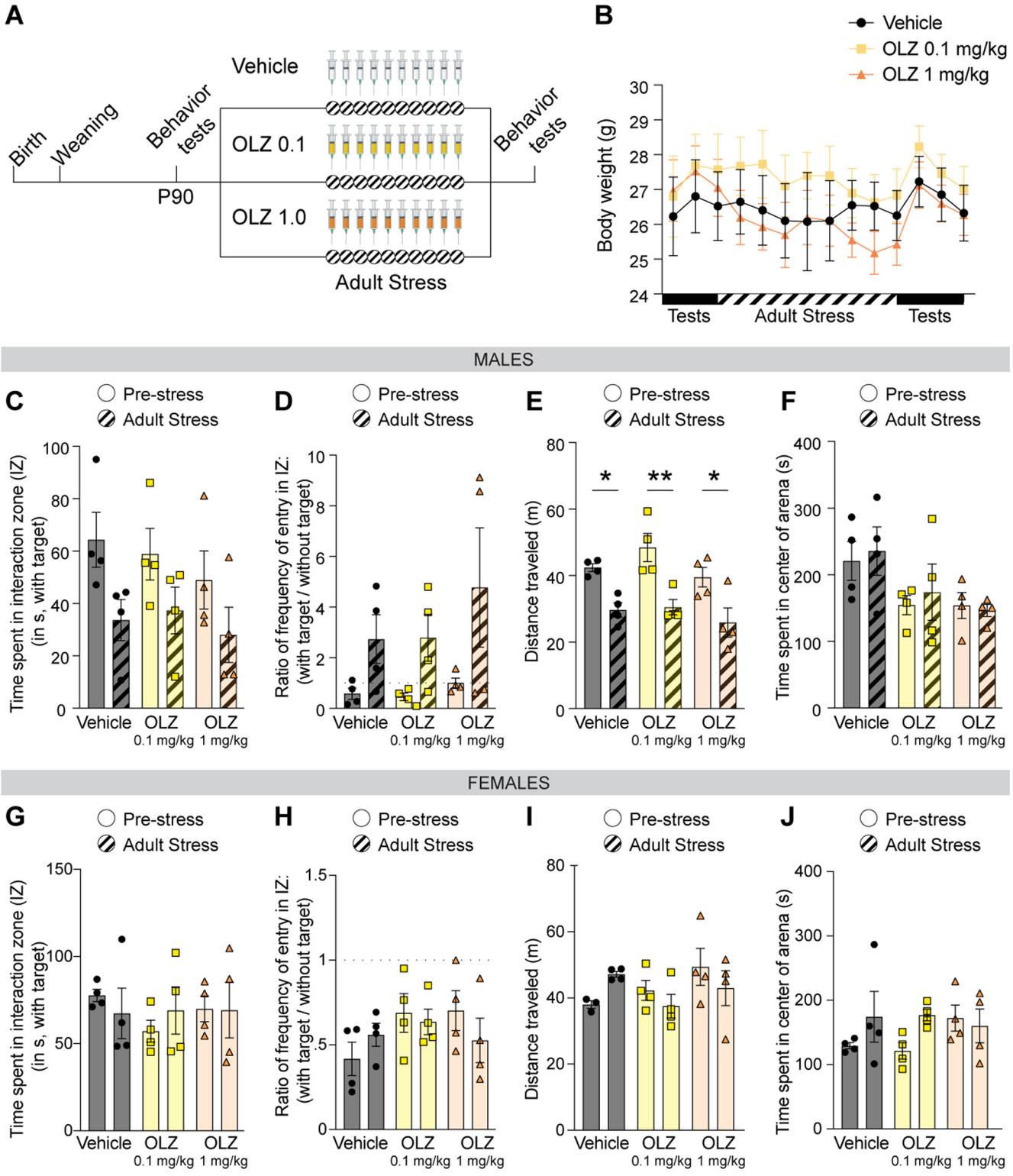

Figure 5. No significant effects of olanzapine treatment by itself on behavior at two doses. ***A***, Schematic of experimental groups: for 10 d, adult wild-type mice underwent male-only CSDS daily, 30 min after receiving an intraperitoneal injection of saline, OLZ (0.1 mg/kg) or OLZ (1 mg/kg). ***B***, No weight change was observed among males after 10 d of OLZ injection at either dose selected. ***C–F***, In the social interaction test, there were no significant differences between treatment groups in either the time spent in interaction zone (***C***) or the frequency of entry in the interaction zone (***D***). In the open-field test, all the mice traveled significantly less after defeat (***E***), but there were no significant differences in time spent in the arena center (***F***). ***G***, ***H***, In female mice, no significant differences were observed in the social interaction test either in the time spent in interaction zone (***G***), or in the frequency of entry in the zone (***H***). ***I***, ***J***, There were also no differences in the total distance traveled (***I***) or in the time spent in the arena center (***J***) in the open-field test. Data are mean ± SEM. *$p < 0.05$, **$p < 0.01$.

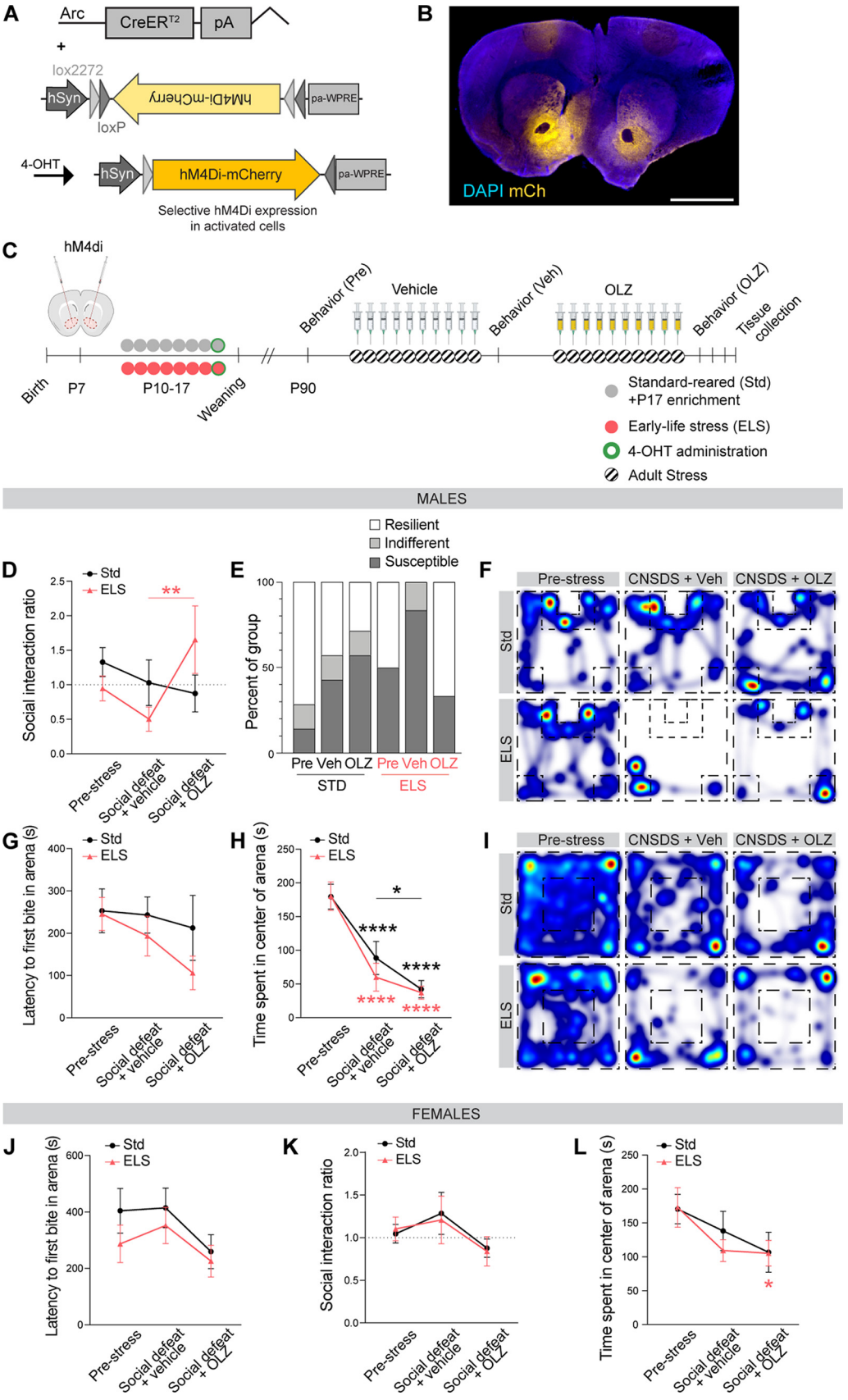

Figure 6. Inhibition of early-life stress-activated cells in NAc reduces hypersensitivity to adult stress in male mice, but not in female mice. ***A***, Viral expression strategy: the administration of 4-OHT to Arc-CreERT2/+ mice injected with AAV-hSyn-hM4Di-mCherry results in permanent hM4Di expression in experience-activated cells. ***B***, Representative image of DREADD-mCherry expression in NAc from pups infused with virus on P7 shows relative specificity of injection even within pups. Scale bar, 2 mm. ***C***, Timeline and experimental groups: mice were either reared in standard conditions or subjected to ELS from P10 to P17. Std-reared mice were given access to a running wheel before 4-OHT-induced recombination on P17. In adulthood, all mice underwent

to stress across the life span and contribute to behavioral stress sensitivity.

Context and time are both essential factors in the retrieval of cellular memories. Neuronal ensembles active in one context—whether a portion of a maze or shock-paired chamber—are less likely to be active in a distinct context (O'Keefe and Nadel, 1978; Josselyn et al., 2015; Moser et al., 2015; Tonegawa et al., 2015a; Cai et al., 2016). Time also erodes memory: an identical context reactivates hippocampal ensembles more at 5 d than at 30 d after the initial experience (Denny et al., 2014). Memories of experiences close in time are also more likely to share overlapping neuronal ensembles than experiences separated by a week or more (Cai et al., 2016), and longitudinal calcium recordings of mPFC cells show substantial representational drift of stress-sensitive ensembles across days (Patel et al., 2022), likely because of ensemble destabilization during repeated retrieval (Cho et al., 2021). Given this, the length of time between initial ELS and adult stress exposures, and the different contexts in which each stress was experienced would predict low reactivation of ELS-sensitive cells in the current study. Nevertheless, we found a similar percentage of reactivation of neurons between ELS and adult CNSDS (~5–15%, depending on brain region) as fear-conditioning studies find in hippocampus (~5%) and amygdala (~10–15%; Denny et al., 2014; DeNardo et al., 2019). This enduring encoding of ELS may therefore contribute to stress hypersensitivity.

While we specifically sought to understand how ELS primes cellular responses to adult stress, another important question concerns the stability of ensembles of ELS-activated cells across days of ELS. Earlier work found similar increases in serum corticosterone following a single bout of maternal separation compared with repeated maternal separation from P1 to P14 or P14 to P21, suggesting that pups do not habituate their hormonal stress response from across days of ELS (Horii-Hayashi et al., 2013; Nishi et al., 2013). We similarly found a high c-Fos response to ELS on P17 with (chronic) or without (acute) prior ELS (Fig. 2*B*). Interestingly in adults, mPFC ensembles tagged at the end of fear conditioning are more likely to be reactivated and contribute to behavior, even at remote time points, than those tagged during early stages of learning (DeNardo et al., 2019). Our choice to tag cells on the last day of ELS therefore likely captured cells most robustly activated across all days of ELS. Finally, we found a higher percentage of c-Fos$^+$ cells on the last day of ELS that were also active on the first day of ELS compared with a low percentage of overlap if early experience was mismatched (Fig. 2*C*), indicating that even while homecage enrichment experience engaged a similar number of neurons across brain regions compared with ELS (Fig. 4), these early-life experiences engaged distinct neuronal ensembles.

Heightened neuronal excitability biases recruitment into ensembles (Kida et al., 2002; Han et al., 2008; Sekeres et al., 2010; Kim et al., 2014; Yiu et al., 2014). ELS did not increase c-Fos-expressing cells at baseline in any brain region (Fig. 4*B*,*F*,*J*,*N*, control) or reactivation of ELS ensembles in the absence of adult stress (Fig. 4*C*,*G*,*K*,*O*, control). Interestingly, in some regions, ELS-exposed mice had lower c-Fos density and overlap than Std-reared mice. It is possible that Std-tagged cells that are active during a positive-valence enrichment experience are more likely to overlap with random homecage activity in adulthood, and that ELS-tagged cells are less likely to be active during homecage exploration; both the lower control levels and higher CNSDS reactivation of ELS-tagged cells indicate specificity. A lack of continual hyperactivity across the life span is also consistent with the idea that ELS ensembles are dormant or even suppressed below baseline outside of retrieval by additional stress (Josselyn et al., 2015). Even dormant ensembles have been shown to facilitate response to stimuli through strengthened synaptic connectivity, glutamate receptor and CREB expression, or by enduring epigenetic mechanisms (Kida et al., 2002; Han et al., 2008; Sekeres et al., 2010; Kim et al., 2014; Yiu et al., 2014; Marco et al., 2020). It will be important for future research to investigate which molecular mechanisms ELS-reactivated neurons engage for sensitized stress response.

We found an interaction between ELS and adult stress on neuronal reactivation within both NAc and mPFC, suggesting that multiple brain regions may contribute to hypersensitivity to adult stress. We chose to manipulate ELS-activated cells in NAc, as NAc integrates glutamatergic inputs from mPFC and BLA and dopaminergic inputs from VTA (French and Totterdell, 2002, 2003; Goto and Grace, 2008; Britt et al., 2012; Bagot et al., 2015; Ramirez et al., 2015). It is possible that manipulating the activity of ELS-activated and enrichment-activated cells upstream of NAc, in mPFC or BLA, would similarly result in behavioral rescue. Indeed, optogenetic inhibition of BLA in ELS-exposed juvenile mice promotes social behavior (Opendak et al., 2021). However, broad inhibition of all glutamatergic activity by optogenetically induced LTD in mPFC or amygdala projections to NAc before behavioral testing did not alter susceptibility or resilience following adult social defeat stress (Bagot et al., 2015).

Chemogenetic inhibition of ELS-activated NAc neurons, but not control-tagged neurons, rescued social avoidance behavior following CNSDS in males (Fig. 6*D–F*). To control for the effects of vehicle versus ligand within subject, mice were exposed to CNSDS twice: first with vehicle administration wherein all mice were assumed to experience the full stress, and again with the DREADD ligand administered daily before each defeat stress exposure. We reasoned that it would be more challenging to rescue behavior after mice had already experienced social defeat and displayed stress-related behavioral changes. While the strongest effect of inhibition was on social avoidance behavior, latency to eat in a novelty-suppressed feeding task appeared to be selectively reduced by DREADD inhibition in ELS males and not Std males. Effective rescue of social avoidance behavior in males and the proportion of mice considered susceptible supports an enduring functional role for ELS-activated NAc neurons in ELS-induced stress hypersensitivity.

While our imaging findings include both males and females, and female ELS-exposed mice appear to respond to CNSDS by reduced open-field center time, NAc ensemble inhibition did not

←

two rounds of CNSDS for 10 d. During the first round, all mice received a vehicle injection 30 min prior to each daily bout of social defeat; in the second round, all mice received 0.1 mg/kg OLZ 30 min prior to social defeat. The sensory period of CNSDS (cohousing across a barrier from an aggressor) was shortened to 3–4 h after defeat instead of overnight to account for the OLZ half-life. Mice were assessed behaviorally before and after each round of CNSDS. ***D***, Social avoidance among male mice, presented as a social interaction ratio, where a lower ratio is associated with greater social avoidance. ***E***, Percentage of male mice categorized as resilient, indifferent, or susceptible to CNSDS under each treatment condition. ***F***, Representative heat maps of average mouse behavior in each group during social interaction testing with an aggressor present. ***G***, Latency of male mice to eat in a novel arena during a novelty-suppressed feeding test. ***H***, Time spent in the center during open-field testing among male mice. ***I***, Representative heat maps of average mouse behavior in each group during open-field exploration. ***J***, Latency of female mice to eat in a novel arena during a novelty-suppressed feeding test. ***K***, Social avoidance among female mice, where a lower social interaction ratio is associated with greater social avoidance. ***L***, Time spent in the center during open-field testing among female mice. OLZ indicates DREADD inhibition of early experience-activated cells. Data are mean ± SEM. *Post hoc* comparisons between corresponding conditions and prestress data are indicated by $^*p < 0.05$, $^{**}p < 0.01$, and $^{****}p < 0.0001$.

affect female behavior across three tests. Recent machine learning-based analysis of female behavior during social defeat attacks also shows relatively more subtle behavioral responses to defeat compared with males (Willmore et al., 2022). Additional research is needed to determine whether distinct adult stressors would produce a stronger effect in females and whether other brain regions, such as within the hypothalamus, more robustly encode female cellular memory of ELS.

Heterogeneity of neuronal subtypes in NAc and other brain regions is important to consider, as Drd1-expressing and Drd2-expressing medium spiny neurons (D1-MSNs and D2-MSNs) contribute to different aspects of behavior. D1-MSNs are classically thought to encode reward signals, and D2-MSNs to encode aversive signals, although this notion has been challenged (Hikida et al., 2010; Kravitz et al., 2012; Kupchik et al., 2015; Soares-Cunha et al., 2020). While we took an activity-dependent rather than a molecularly defined approach and did not distinguish between D1-MSNs and D2-MSNs in NAc in the current study, recent work found that ELS predominately impacts the molecular profiles of D2-MSNs in NAc (Kronman et al., 2021). Consistent with an hypothesis that ELS predominantly acts on D2-MSNS, adult stress in male mice has been found to increase excitatory transmission onto D2-MSNs and to decrease excitatory transmission onto D1-MSNs (Francis et al., 2015). While inhibiting D1-MSNs in stress-resilient mice increases depression-like behavior and activating D2-MSNs before stress increases susceptibility, the effect of inhibiting D2-MSNs specifically during stress experience has not yet been reported and would be an important follow-up for the current study (Francis et al., 2015; Peña, 2017). These previous studies showing D2-MSN activation-induced stress susceptibility suggests that activating ELS-activated cells with an excitatory DREADD would be sufficient to sensitize mice to subthreshold stress, but additional studies are needed to confirm.

Another remaining question is how generalizable these results are to other types of stress, such as nonsocial stress. In an unpublished experiment, we found similar levels and fold change of Fos^+ cells in NAc in response to both adult social defeat and 1 week of unpredictable chronic mild stress, and similar fold change in Fos^+ cells between Std and ELS mice in other brain regions [our unpublished observations (for lack of specific Sun1 tagging in Std-mice)]. The generalizability of the response to distinct stressors is in line with previous research describing distinct NAc circuitry for response to rewarding and aversive stimuli (Hikida et al., 2010). However, a true stress "labeled line" model might predict a greater percentage reactivation of ELS^+ cells as generic stress-responsive cells and does not account for the increase in Fos^+ cells and colabeled cells after ELS and adult stress that we observe. Nonetheless, it would be interesting for future studies to directly compare reactivation of NAc cells across distinct adult stressors.

In sum, these data provide evidence that NAc neuronal ensembles encode ELS-induced stress hypersensitivity. This work paves the way for additional research to understand how ELS activation alters the molecular development and circuit integration of corticolimbic neurons, and to formulate translational strategies to ameliorate stress hypersensitivity in individuals who experienced ELS and are at risk for developing mood and anxiety disorders.

References

Alper K, Schwartz KA, Kolts RL, Khan A (2007) Seizure incidence in psychopharmacological clinical trials: an analysis of Food and Drug Administration (FDA) summary basis of approval reports. Biol Psychiatry 62:345–354.

Aravagiri M, Teper Y, Marder SR (1999) Pharmacokinetics and tissue distribution of olanzapine in rats. Biopharm Drug Dispos 20:369–377.

Bagot RC, Parise EM, Peña CJ, Zhang H-X, Maze I, Chaudhury D, Persaud B, Cachope R, Bolaños-Guzmán CA, Cheer JF, Cheer J, Deisseroth K, Han M-H, Nestler EJ (2015) Ventral hippocampal afferents to the nucleus accumbens regulate susceptibility to depression. Nat Commun 6:7062.

Berton O, McClung CA, DiLeone RJ, Krishnan V, Renthal W, Russo SJ, Graham D, Tsankova NM, Bolanos CA, Rios M, Monteggia LM, Self DW, Nestler EJ (2006) Essential role of BDNF in the mesolimbic dopamine pathway in social defeat stress. Science 311:864–868.

Bodnoff SR, Suranyi-Cadotte B, Quirion R, Meaney MJ (1989) A comparison of the effects of diazepam versus several typical and atypical anti-depressant drugs in an animal model of anxiety. Psychopharmacology (Berl) 97:277–279.

Britt JP, Benaliouad F, McDevitt RA, Stuber GD, Wise RA, Bonci A (2012) Synaptic and behavioral profile of multiple glutamatergic inputs to the nucleus accumbens. Neuron 76:790–803.

Butler CW, Wilson YM, Gunnersen JM, Murphy M (2015) Tracking the fear memory engram: discrete populations of neurons within amygdala, hypothalamus, and lateral septum are specifically activated by auditory fear conditioning. Learn Mem Cold Mem 22:370–384.

Cai DJ, et al. (2016) A shared neural ensemble links distinct contextual memories encoded close in time. Nature 534:115–118.

Cho H-Y, Shin W, Lee H-S, Lee Y, Kim M, Oh J-P, Han J, Jeong Y, Suh B, Kim E, Han J-H (2021) Turnover of fear engram cells by repeated experience. Curr Biol 31:5450–5461.e4.

Cowansage KK, Shuman T, Dillingham BC, Chang A, Golshani P, Mayford M (2014) Direct reactivation of a coherent neocortical memory of context. Neuron 84:432–441.

Davis P, Reijmers LG (2018) The dynamic nature of fear engrams in the basolateral amygdala. Brain Res Bull 141:44–49.

DeNardo D, Liu CD, Allen WE, Adams EL, Friedmann D, Fu L, Guenthner CJ, Tessier-Lavigne M, Luo L (2019) Temporal evolution of cortical ensembles promoting remote memory retrieval. Nat Neurosci 22:460–469.

DeNardo L, Luo L (2017) Genetic strategies to access activated neurons. Curr Opin Neurobiol 45:121–129.

Deng W, Mayford M, Gage FH (2013) Selection of distinct populations of dentate granule cells in response to inputs as a mechanism for pattern separation in mice. eLife 2:e00312.

Denny CA, Kheirbek MA, Alba EL, Tanaka KF, Brachman RA, Laughman KB, Tomm NK, Turi GF, Losonczy A, Hen R (2014) Hippocampal memory traces are differentially modulated by experience, time, and adult neurogenesis. Neuron 83:189–201.

Deroulers C, Ameisen D, Badoual M, Gerin C, Granier A, Lartaud M (2013) Analyzing huge pathology images with open source software. Diagn Pathol 8:92.

Dieterich A, Liu T, Samuels BA (2021) Chronic non-discriminatory social defeat stress reduces effort-related motivated behaviors in male and female mice. Transl Psychiatry 11:125.

Dunn EC, Nishimi K, Gomez SH, Powers A, Bradley B (2018) Developmental timing of trauma exposure and emotion dysregulation in adulthood: are there sensitive periods when trauma is most harmful? J Affect Disord 227:869–877.

Dunn EC, Soare TW, Zhu Y, Simpkin AJ, Suderman MJ, Klengel T, Smith ADAC, Ressler KJ, Relton CL (2019) Sensitive periods for the effect of childhood adversity on DNA methylation: results from a prospective, longitudinal study. Biol Psychiatry 85:838–849.

Francis TC, Chandra R, Friend DM, Finkel E, Dayrit G, Miranda J, Brooks JM, Iñiguez SD, O'Donnell P, Kravitz A, Lobo MK (2015) Nucleus accumbens medium spiny neuron subtypes mediate depression-related outcomes to social defeat stress. Biol Psychiatry 77:212–222.

French SJ, Totterdell S (2002) Hippocampal and prefrontal cortical inputs monosynaptically converge with individual projection neurons of the nucleus accumbens. J Comp Neurol 446:151–165.

French SJ, Totterdell S (2003) Individual nucleus accumbens-projection neurons receive both basolateral amygdala and ventral subicular afferents in rats. Neuroscience 119:19–31.

Gomez JL, Bonaventura J, Lesniak W, Mathews WB, Sysa-Shah P, Rodriguez LA, Ellis RJ, Richie CT, Harvey BK, Dannals RF, Pomper MG, Bonci A,

Michaelides M (2017) Chemogenetics revealed: DREADD occupancy and activation via converted clozapine. Science 357:503–507.
Goto Y, Grace AA (2008) Limbic and cortical information processing in the nucleus accumbens. Trends Neurosci 31:552–558.
Green JG, McLaughlin KA, Berglund PA, Gruber MJ, Sampson NA, Zaslavsky AM, Kessler RC (2010) Childhood adversities and adult psychiatric disorders in the national comorbidity survey replication I: associations with first onset of DSM-IV disorders. Arch Gen Psychiatry 67:113–123.
Guzowski JF, McNaughton BL, Barnes CA, Worley PF (1999) Environment-specific expression of the immediate-early gene Arc in hippocampal neuronal ensembles. Nat Neurosci 2:1120–1124.
Han J-H, Kushner SA, Yiu AP, Cole CJ, Matynia A, Brown RA, Neve RL, Guzowski JF, Silva AJ, Josselyn SA (2007) Neuronal competition and selection during memory formation. Science 316:457–460.
Han J-H, Kushner SA, Yiu AP, Hsiang H-LL, Buch T, Waisman A, Bontempi B, Neve RL, Frankland PW, Josselyn SA (2009) Selective erasure of a fear memory. Science 323:1492–1496.
Han J-H, Yiu AP, Cole CJ, Hsiang H-L, Neve RL, Josselyn SA (2008) Increasing CREB in the auditory thalamus enhances memory and generalization of auditory conditioned fear. Learn Mem Cold Mem 15:443–453.
Hanson JL, Williams AV, Bangasser DA, Peña CJ (2021) Impact of early life stress on reward circuit function and regulation. Front Psychiatry 12:744690.
Hikida T, Kimura K, Wada N, Funabiki K, Nakanishi S (2010) Distinct roles of synaptic transmission in direct and indirect striatal pathways to reward and aversive behavior. Neuron 66:896–907.
Horii-Hayashi N, Sasagawa T, Matsunaga W, Matsusue Y, Azuma C, Nishi M (2013) Developmental changes in desensitisation of c-Fos expression induced by repeated maternal separation in pre-weaned mice. J Neuroendocrinol 25:158–167.
Hsiang H-LL, Epp JR, van den Oever MC, Yan C, Rashid AJ, Insel N, Ye L, Niibori Y, Deisseroth K, Frankland PW, Josselyn SA (2014) Manipulating a "cocaine engram" in mice. J Neurosci 34:14115–14127.
Janak PH, Tye KM (2015) From circuits to behaviour in the amygdala. Nature 517:284–292.
Josselyn SA, Köhler S, Frankland PW (2015) Finding the engram. Nat Rev Neurosci 16:521–534.
Kida S, Josselyn SA, Peña de Ortiz S, Kogan JH, Chevere I, Masushige S, Silva AJ (2002) CREB required for the stability of new and reactivated fear memories. Nat Neurosci 5:348–355.
Kim J, Kwon J-T, Kim H-S, Josselyn SA, Han J-H (2014) Memory recall and modifications by activating neurons with elevated CREB. Nat Neurosci 17:65–72.
Kitamura T, Ogawa SK, Roy DS, Okuyama T, Morrissey MD, Smith LM, Redondo RL, Tonegawa S (2017) Engrams and circuits crucial for systems consolidation of a memory. Science 356:73–78.
Krashes MJ, Koda S, Ye C, Rogan SC, Adams AC, Cusher DS, Maratos-Flier E, Roth BL, Lowell BB (2011) Rapid, reversible activation of AgRP neurons drives feeding behavior in mice. J Clin Invest 121:1424–1428.
Kravitz AV, Tye LD, Kreitzer AC (2012) Distinct roles for direct and indirect pathway striatal neurons in reinforcement. Nat Neurosci 15:816–818.
Krishnan V, et al. (2007) Molecular adaptations underlying susceptibility and resistance to social defeat in brain reward regions. Cell 131:391–404.
Kronman H, Torres-Berrío A, Sidoli S, Issler O, Godino A, Ramakrishnan A, Mews P, Lardner CK, Parise EM, Walker DM, van der Zee YY, Browne CJ, Boyce BF, Neve R, Garcia BA, Shen L, Peña CJ, Nestler EJ (2021) Long-term behavioral and cell-type-specific molecular effects of early life stress are mediated by H3K79me2 dynamics in medium spiny neurons. Nat Neurosci 24:667–676.
Kupchik YM, Brown RM, Heinsbroek JA, Lobo MK, Schwartz DJ, Kalivas PW (2015) Coding the direct/indirect pathways by D1 and D2 receptors is not valid for accumbens projections. Nat Neurosci 18:1230–1232.
Lieb A, Weston M, Kullmann DM (2019) Designer receptor technology for the treatment of epilepsy. EBioMedicine 43:641–649.
Liu X, Ramirez S, Pang PT, Puryear CB, Govindarajan A, Deisseroth K, Tonegawa S (2012) Optogenetic stimulation of a hippocampal engram activates fear memory recall. Nature 484:381–385.
Loryan I, Melander E, Svensson M, Payan M, König F, Jansson B, Hammarlund-Udenaes M (2016) In-depth neuropharmacokinetic analysis of antipsychotics based on a novel approach to estimate unbound target-site concentration in CNS regions: link to spatial receptor occupancy. Mol Psychiatry 21:1527–1536.
Marco A, Meharena HS, Dileep V, Raju RM, Davila-Velderrain J, Zhang AL, Adaikkan C, Young JZ, Gao F, Kellis M, Tsai L-H (2020) Mapping the epigenomic and transcriptomic interplay during memory formation and recall in the hippocampal engram ensemble. Nat Neurosci 23:1606–1617.
Matos MR, Visser E, Kramvis I, van der Loo RJ, Gebuis T, Zalm R, Rao-Ruiz P, Mansvelder HD, Smit AB, van den Oever MC (2019) Memory strength gates the involvement of a CREB-dependent cortical fear engram in remote memory. Nat Commun 10:2315.
Mattiuz E, Franklin R, Gillespie T, Murphy A, Bernstein J, Chiu A, Hotten T, Kassahun K (1997) Disposition and metabolism of olanzapine in mice, dogs, and rhesus monkeys. Drug Metab Dispos 25:573–583.
McKenzie S, Frank AJ, Kinsky NR, Porter B, Rivière PD, Eichenbaum H (2014) Hippocampal representation of related and opposing memories develop within distinct, hierarchically organized neural schemas. Neuron 83:202–215.
McLaughlin KA, Kubzansky LD, Dunn EC, Waldinger R, Vaillant G, Koenen KC (2010) Childhood social environment, emotional reactivity to stress, and mood and anxiety disorders across the life course. Depress Anxiety 27:1087–1094.
Mo A, Mukamel EA, Davis FP, Luo C, Henry GL, Picard S, Urich MA, Nery JR, Sejnowski TJ, Lister R, Eddy SR, Ecker JR, Nathans J (2015) Epigenomic signatures of neuronal diversity in the mammalian brain. Neuron 86:1369–1384.
Moser M-B, Rowland DC, Moser EI (2015) Place cells, grid cells, and memory. Cold Spring Harb Perspect Biol 7:a021808.
Nishi M, Horii-Hayashi N, Sasagawa T, Matsunaga W (2013) Effects of early life stress on brain activity: implications from maternal separation model in rodents. Gen Comp Endocrinol 181:306–309.
O'Keefe J, Nadel L (1978) The hippocampus as a cognitive map. Oxford, UK/New York: Clarendon Press/Oxford UP.
Okuyama T, Kitamura T, Roy DS, Itohara S, Tonegawa S (2016) Ventral CA1 neurons store social memory. Science 353:1536–1541.
Opendak M, Raineki C, Perry RE, Rincón-Cortés M, Song SC, Zanca RM, Wood E, Packard K, Hu S, Woo J, Martinez K, Vinod KY, Brown RW, Deehan GA, Froemke RC, Serrano PA, Wilson DA, Sullivan RM (2021) Bidirectional control of infant rat social behavior via dopaminergic innervation of the basolateral amygdala. Neuron 109:4018–4035.e7.
Pastuzyn ED, Day CE, Kearns RB, Kyrke-Smith M, Taibi AV, McCormick J, Yoder N, Belnap DM, Erlendsson S, Morado DR, Briggs JAG, Feschotte C, Shepherd JD (2018) The neuronal gene arc encodes a repurposed retrotransposon Gag protein that mediates intercellular RNA transfer. Cell 172:275–288.e18.
Patel S, Johnson K, Adank D, Rosas-Vidal LE (2022) Longitudinal monitoring of prefrontal cortical ensemble dynamics reveals new insights into stress habituation. Neurobiol Stress 20:100481.
Peña CJ (2017) D1 and D2 type medium spiny neuron contributions to depression. Biol Psychiatry 81:636–638.
Peña CJ, Kronman HG, Walker DM, Cates HM, Bagot RC, Purushothaman I, Issler O, Loh Y-HE, Leong T, Kiraly DD, Goodman E, Neve RL, Shen L, Nestler EJ (2017) Early life stress confers lifelong stress susceptibility in mice via ventral tegmental area OTX2. Science 356:1185–1188.
Peña CJ, Smith M, Ramakrishnan A, Cates HM, Bagot RC, Kronman HG, Patel B, Chang AB, Purushothaman I, Dudley J, Morishita H, Shen L, Nestler EJ (2019) Early life stress alters transcriptomic patterning across reward circuitry in male and female mice. Nat Commun 10:5098.
Pignatelli M, Ryan TJ, Roy DS, Lovett C, Smith LM, Muralidhar S, Tonegawa S (2019) Engram cell excitability state determines the efficacy of memory retrieval. Neuron 101:274–284.e5.
Ramirez S, Liu X, Lin P-A, Suh J, Pignatelli M, Redondo RL, Ryan TJ, Tonegawa S (2013) Creating a false memory in the hippocampus. Science 341:387–391.
Ramirez S, Liu X, MacDonald CJ, Moffa A, Zhou J, Redondo RL, Tonegawa S (2015) Activating positive memory engrams suppresses depression-like behaviour. Nature 522:335–339.
Redondo RL, Kim J, Arons AL, Ramirez S, Liu X, Tonegawa S (2014) Bidirectional switch of the valence associated with a hippocampal contextual memory engram. Nature 513:426–430.
Roy DS, Park Y-G, Kim ME, Zhang Y, Ogawa SK, DiNapoli N, Gu X, Cho JH, Choi H, Kamentsky L, Martin J, Mosto O, Aida T, Chung K,

Tonegawa S (2022) Brain-wide mapping reveals that engrams for a single memory are distributed across multiple brain regions. Nat Commun 13:1799.

Russo SJ, Nestler EJ (2013) The brain reward circuitry in mood disorders. Nat Rev Neurosci 14:609–625.

Ryan TJ, Roy DS, Pignatelli M, Arons A, Tonegawa S (2015) Engram cells retain memory under retrograde amnesia. Science 348:1007–1013.

Saxton K, Chyu L (2020) Early life adversity increases the salience of later life stress: an investigation of interactive effects in the PSID. J Dev Orig Health Dis 11:25–36.

Scott KM, McLaughlin KA, Smith DAR, Ellis PM (2012) Childhood maltreatment and DSM-IV adult mental disorders: comparison of prospective and retrospective findings. Br J Psychiatry J Psychiatry 200:469–475.

Sekeres MJ, Neve RL, Frankland PW, Josselyn SA (2010) Dorsal hippocampal CREB is both necessary and sufficient for spatial memory. Learn Mem Cold Mem 17:280–283.

Shertzer HG, Kendig EL, Nasrallah HA, Johansson E, Genter MB (2010) Protection from olanzapine-induced metabolic toxicity in mice by acetaminophen and tetrahydroindenoindole. Int J Obes (Lond) 34:970–979.

Shpokayte M, McKissick O, Guan X, Yuan B, Rahsepar B, Fernandez FR, Ruesch E, Grella SL, White JA, Liu XS, Ramirez S (2022) Hippocampal cells segregate positive and negative engrams. Commun Biol 5:1009.

Sidamon-Eristoff AE, Cohodes EM, Gee DG, Peña CJ (2022) Trauma exposure and mental health outcomes among Central American and Mexican children held in immigration detention at the United States-Mexico border. Dev Psychobiol 64:e22227.

Soares-Cunha C, de Vasconcelos NAP, Coimbra B, Domingues AV, Silva JM, Loureiro-Campos E, Gaspar R, Sotiropoulos I, Sousa N, Rodrigues AJ (2020) Nucleus accumbens medium spiny neurons subtypes signal both reward and aversion. Mol Psychiatry 25:3241–3255.

Tonegawa S, Liu X, Ramirez S, Redondo R (2015a) Memory Engram Cells Have Come of Age. Neuron 87:918–931.

Tonegawa S, Pignatelli M, Roy DS, Ryan TJ (2015b) Memory engram storage and retrieval. Curr Opin Neurobiol 35:101–109.

Upright NA, Baxter MG (2020) Effect of chemogenetic actuator drugs on prefrontal cortex-dependent working memory in nonhuman primates. Neuropsychopharmacology 45:1793–1798.

van der Zwaal EM, Janhunen SK, la Fleur SE, Adan RAH (2014) Modelling olanzapine-induced weight gain in rats. Int J Neuropsychopharmacol 17:169–186.

Wang J-S, Taylor R, Ruan Y, Donovan JL, Markowitz JS, Lindsay De Vane C (2004) Olanzapine penetration into brain is greater in transgenic Abcb1a P-glycoprotein-deficient mice than FVB1 (wild-type) animals. Neuropsychopharmacology 29:551–557.

Weston M, Kaserer T, Wu A, Mouravlev A, Carpenter JC, Snowball A, Knauss S, von Schimmelmann M, During MJ, Lignani G, Schorge S, Young D, Kullmann DM, Lieb A (2019) Olanzapine: a potent agonist at the hM4D(Gi) DREADD amenable to clinical translation of chemogenetics. Sci Adv 5:eaaw1567.

Willmore L, Cameron C, Yang J, Witten IB, Falkner AL (2022) Behavioural and dopaminergic signatures of resilience. Nature 611:124–132.

Yiu AP, Mercaldo V, Yan C, Richards B, Rashid AJ, Hsiang H-LL, Pressey J, Mahadevan V, Tran MM, Kushner SA, Woodin MA, Frankland PW, Josselyn SA (2014) Neurons are recruited to a memory trace based on relative neuronal excitability immediately before training. Neuron 83:722–735.

Yohn CN, Dieterich A, Bazer AS, Maita I, Giedraitis M, Samuels BA (2019) Chronic non-discriminatory social defeat is an effective chronic stress paradigm for both male and female mice. Neuropsychopharmacology 44:2220–2229.

Zhang Z-Y, Mao Y, Feng X-L, Zheng N, Lü L-B, Ma Y-Y, Qin D-D, Hu X-T (2016) Early adversity contributes to chronic stress induced depression-like behavior in adolescent male rhesus monkeys. Behav Brain Res 306:154–159.

Zhou Y, Zhu H, Liu Z, Chen X, Su X, Ma C, Tian Z, Huang B, Yan E, Liu X, Ma L (2019) A ventral CA1 to nucleus accumbens core engram circuit mediates conditioned place preference for cocaine. Nat Neurosci 22:1986–1999.